

## Mechanics of Binding of a Single Integration-Host-Factor Protein to DNA

Sanhita Dixit, Mukta Singh-Zocchi, Jeungphill Hanne, and Giovanni Zocchi

Department of Physics and Astronomy, University of California, Los Angeles, Los Angeles, California 90095-1547, USA

(Received 6 October 2004; published 22 March 2005)

We report on a single-molecule experiment where we directly observe local bending of a 76 base pair DNA oligomer caused by specific binding of a single integration-host-factor (IHF) protein. The conformational change of the DNA is detected by optically monitoring the displacement of a micron size bead tethered to a surface by the DNA. Since in the bound state the DNA loops around the IHF, a mechanical tension on the DNA tends to eject the protein. We measure how the rate for the protein to fall off the DNA depends on the mechanical tension in the DNA, gaining insight into the energy landscape for this molecular bond. Our method further demonstrates a new paradigm of molecular detection, where ligand binding is detected through the conformational change induced in the probe molecule. Here this allows the detection of single, unlabeled proteins.

DOI: 10.1103/PhysRevLett.94.118101

PACS numbers: 87.15.He

**Introduction.**—DNA binding proteins can induce substantial deformations of the DNA, because binding energies are comparable to the work required to locally bend or twist the DNA. An example which is studied in atomic detail is the IHF (integration-host-factor) protein of *E. coli*, which is involved in the mechanism of integration of the bacteriophage  $\lambda$  DNA into the *E. coli* chromosome. The crystallographic structure of the complex shows the DNA bent into a half circle around the protein [1]. The natural tool to study such large molecular deformations is *force spectroscopy*, where a mechanical force couples to the conformational change. This approach has been demonstrated through single-molecule experiments on motor proteins [2,3] and DNA-modifying enzymes including polymerases [4,5] and topoisomerases [6]. Large-scale DNA looping, induced by regulatory factors such as Lac repressor, has been studied in real time by detecting the shortening of the end-to-end distance (EED) of a single 1 kb long DNA molecule resulting from the loop caused by the protein binding [7]. Similar experiments can detect the overall compaction of the DNA when many IHF proteins bind [8]. But in order to see single, local bending events, one has to work with DNA at the  $\sim 10$  nm scale.

Here we detect in real time local bending of a single 25 nm long DNA molecule caused by single IHF binding events. The experiment allows one to measure directly the relation between DNA tension and protein binding dynamics. Our probe is a  $1\ \mu\text{m}$  size bead tethered to the surface of a microscope slide through a single 76 base pair (bp) long DNA molecule containing a consensus sequence for IHF binding (Fig. 1). We have shown previously that by monitoring the position of the bead relative to the surface we can detect conformational changes in the molecular tether [9]. The bead's position is monitored optically using an evanescent wave scattering method [10]. In addition, by analyzing the thermal motion of the bead we can determine the mechanical tension on the tether [11]. Here we combine these two measurements to explore the relation be-

tween DNA tension and the dynamics of protein binding. We detect single protein binding events from the change in EED of the DNA due to local bending. We measure the lifetime of the bound state and its dependence on DNA tension.

**Results.**—Experiments were conducted as follows. A bead is selected, which, judging from the amplitude of its thermal motion, is attached to the slide surface through a single DNA tether. This is the most probable configuration

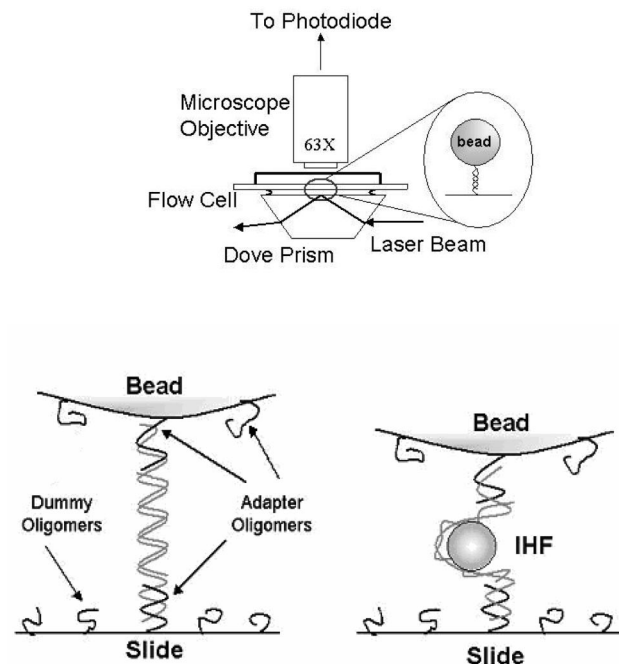


FIG. 1. Top: Schematics of the experimental setup; the bead is tethered to the bottom of the flow cell by the probe DNA; its position is monitored using evanescent wave scattering. Bottom: The 76 bases long probe DNA containing the IHF binding site is grafted to the  $1\ \mu\text{m}$  diameter bead and slid through adapter oligomers. When IHF binds, the bead is pulled towards the slide.

under the low surface density of attachment points used in the sample preparation; furthermore, a bead attached through multiple tethers shows distinctively smaller amplitude motion. The motion of the bead is observed for some 30 min, and then IHF is introduced in the flow cell. We then observe that the system starts switching between two states: the initial state (before IHF was introduced) and a new state characterized by a shorter tether (Fig. 2); this second state corresponds to a single IHF protein bound to the DNA tether, which is bent around the protein. Thus the recording of Fig. 2 shows in real time a single protein molecule binding to and falling off from a 25 nm long piece of DNA, the process being captured by monitoring the change in conformation of the DNA. The observed change in maximum extension of the tether in the bound and unbound states,  $\sim 8$  nm (Fig. 2), is consistent with the geometry of the DNA loop around the protein (Fig. 1): the contour length of the DNA loop is, from the crystal structure, 3 helix turns or  $\sim 10$  nm, and the diameter of the protein is  $\sim 2$  nm, so stretching out the loop increases the EED of the tether by  $\sim 8$  nm.

From these recordings we measure the duration of the bound states; the corresponding cumulative distribution is shown in Fig. 3(a), where the slope of the line in the semilog plot is the inverse of the lifetime of the bound state (the off rate). Figure 3(a) shows that there are two different off rates for IHF, corresponding to two modes of binding. In control experiments where the DNA tether did not contain the binding sequence for IHF, we did not observe any instance of DNA bending.

When the protein binds, the bead is pulled close to the surface (Fig. 1); the DNA tether is then under tension because of the repulsive electrostatic and possibly entropic

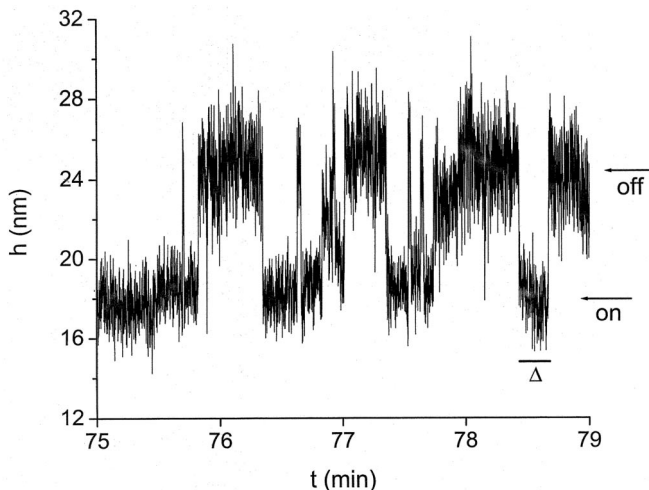


FIG. 2. Time series of the bead's position (in nm) with respect to the surface, showing that single IHF molecules bind to the DNA and fall off. In the bound state, the DNA is bent and the bead is pulled closer to the surface. For each binding event, we can measure the duration of the bound state,  $\Delta$ .

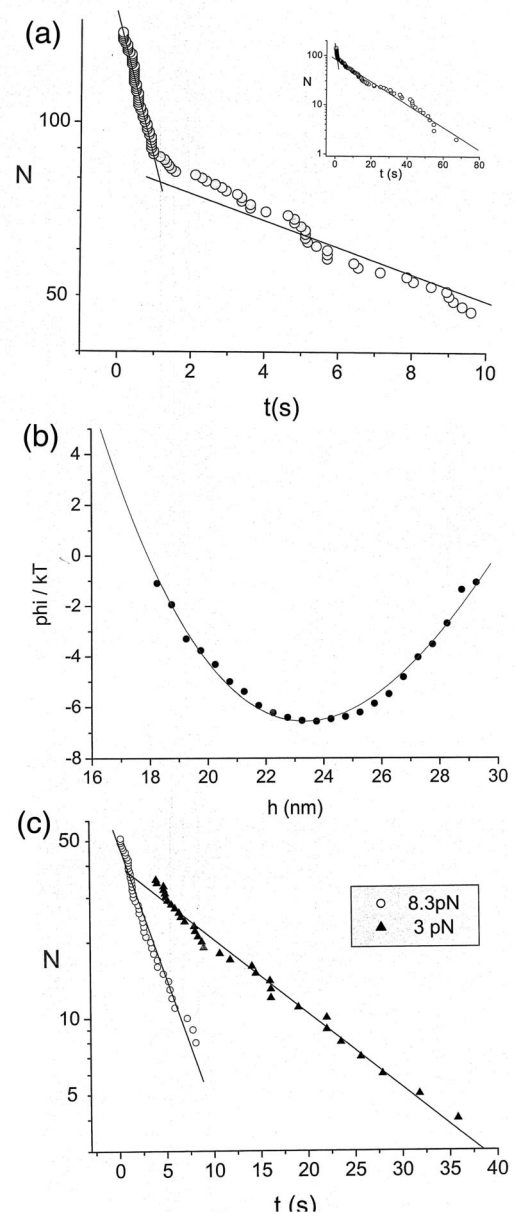


FIG. 3. (a) Cumulative distribution of the duration of the bound state  $\Delta$  obtained from a time trace such as shown in Fig. 2. With a total of  $N(0)$  observed binding events,  $N(0) - N(t)$  is the number of time intervals with  $\Delta < t$ . The slope in a semilog plot gives the off rate. We observe two different off rates [ $(5.3 \pm 0.7) \times 10^{-2} \text{ s}^{-1}$  and  $0.54 \pm 0.10 \text{ s}^{-1}$  in this case], corresponding to two distinct modes of binding of the IHF. The straight lines are linear fits; the whole data set is shown in the inset. (b) The bead-slide interaction potential measured from the thermal motion of the bead in the “off” state. The continuous line is a fit used in the analysis. When the IHF binds, shortening of the molecular tether pulls the bead up the repulsive part of the potential. The derivative of the potential at the “bound” position (see Fig. 2) gives the tension on the tether. (c) Different tensions in the DNA give rise to different off rates. The plot shows the statistics of the “fast” time scale for two different experiments corresponding to measured tensions of 3 and 8.3 pN. The slopes give off rates of  $4.9 \times 10^{-2}$  and  $0.24 \text{ s}^{-1}$ , respectively.

force between the bead and the slide caused by the charged polymers grafted on the surfaces. We measure the tension on the molecular tether by the following method [10,12,13]: we construct the bead-slide interaction potential from the Brownian motion of the bead in the off state (protein not bound) [Fig. 3(b)]. The derivative of the potential at the position corresponding to the on state (protein bound) gives the average tension on the tether. We have shown previously that this method gives quantitatively correct force measurements [11,14]. While we do not control the tension externally (as, for instance, in the atomic force microscope experiments), different realizations of the experiment give rise to different tensions (depending on the nanometer scale surface topography around the grafting site of the tether), and, crucially, we can measure this tension.

In our setup, the forces between the bead and the slide are the following: (1) the repulsive electrostatic and entropic interaction caused by the charged polymers grafted on the surfaces; (2) the attractive van der Waals (vdW) interaction; (3) the DNA tether elasticity. An example of bead-slide interaction potential is shown in Fig. 3(b). The vdW force is small at these distances (e.g., for a  $1\ \mu\text{m}$  bead at  $h = 20\ \text{nm}$ ,  $F_{\text{vdW}} \approx 0.1\ \text{pN}$ ). If  $h_0$  is the position of the minimum of the potential energy [ $h_0 \approx 24\ \text{nm}$  in Fig. 3(b)], for  $h > h_0$  the force on the bead is dominated by the tether elasticity. For a DNA tether of contour length  $L < \ell_p$  (where  $\ell_p$  is the persistence length) the average EED is  $X_{\text{av}} \approx \ell_p[1 - \exp(-L/\ell_p)]$  [15], which in our case ( $L \approx 30\ \text{nm}$ ,  $\ell_p \approx 50\ \text{nm}$ ) gives  $X_{\text{av}} \approx 22\ \text{nm}$  [i.e.,  $L - X_{\text{av}} \approx 8\ \text{nm}$ , which is consistent with the spatial extent of the attractive part of the potential in Fig. 3(b)]. To stretch the DNA beyond  $X_{\text{av}}$  requires a force corresponding to the potential energy surface to the right of the minimum in Fig. 3(b). On the other hand, if the bead-slide separation is less than  $X_{\text{av}}$ , then the force due to the tether is zero, because the tether is attached to the surfaces by freely swiveling joints (i.e., the bead can come close to the surface without bending the tether). Thus the potential energy surface in Fig. 3(b) for  $h < X_{\text{av}} \approx 22$  represents the electrostatic and steric repulsion only (no contribution from the tether elasticity). When the DNA tether is buckled by the protein and pulls the bead near the surface ( $h < X_{\text{av}}$ ), the tether is under tension due to this repulsive force, which in effect has the role of an external field.

In the bound state, the height fluctuations of the bead are reduced (see Fig. 2) for two reasons. First, the repulsive part of the potential is not harmonic (it is roughly exponential), so in the bound state the bead is confined by a steeper potential surface on the left. Second, in the bound state, assuming the protein-DNA complex is stiff, the effective contour length of DNA contributing to the tether elasticity is reduced from  $L \approx 30\ \text{nm}$  to  $L_{\text{bound}} \approx 20\ \text{nm}$ ; referring to the estimate above, we now obtain  $L_{\text{bound}} -$

$X_{\text{av}} \approx 4\ \text{nm}$  so the potential surface to the right of the new equilibrium position is also steeper.

Since in the bound state the DNA forms a loop around the protein, the mechanical tension on the DNA will tend to eject the protein; i.e., it will increase the off rate. Figure 3(c) shows that indeed the off rate is dramatically different for two experiments corresponding to two different tensions. Thus, depending on the mechanical tension, one obtains a whole spectrum of lifetimes for the bound state. Data from several different experiments, including both short and long lifetimes (corresponding to the two modes of binding), are summarized in the graph of Fig. 4. In the simplest model, the off rate  $r(w)$  is given by the Kramers formula for escaping over a barrier [16], with the barrier height diminished by the work  $w$  done by the external force in pulling the particle over the barrier:

$$r(w) = r(0)e^{w/T}, \quad (1)$$

where  $r(0)$  is the off rate at zero external force (as measured in ensemble experiments), and  $T$  is the temperature in energy units. For a uniform external force,  $w = F \times s$ ,

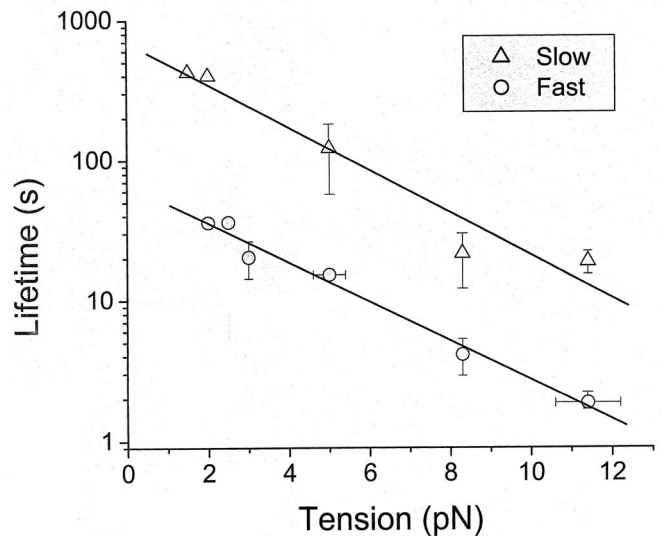


FIG. 4. The lifetime of the IHF bound state vs tension in the DNA for the two different modes of binding. The data are consistent with an exponential dependence on tension. Vertical error bars represent the statistical error originating from the finite sample size and were determined from a simulation (see [19]); the horizontal error bars originate from the spread in the bead's position in the bound state and the uncertainty in the derivative of the potential. The slope of the line is the same for the two modes of binding and defines a characteristic length scale (the position of the barrier in the energy landscape confining the bound state)  $s \approx 1.4 \pm 0.2\ \text{nm}$ . A more detailed analysis, taking into account that the external force varies in space, yields the more accurate values  $s \approx 1.7 \pm 0.2\ \text{nm}$  (see Fig. S3 in the supplementary material [19]). Extrapolating the data to zero tension, we recover the life times measured in ensemble experiments.

where the characteristic length scale  $s$  represents the position in the energy landscape of the top of the barrier which confines the bound state. This parameter has been measured (though not for this system) from the dependence on the pulling rate of the force necessary to break a bond [17,18]. Here we estimate it from the semilog plot of Fig. 4, which is consistent with an exponential dependence on the tension:  $r(F) = r(0) \exp(F \times s/T)$ ; from the slope of the graphs, we extract  $s \approx 1.4 \pm 0.2$  nm. A more detailed analysis (see [19]), taking into account that in our case the force is not constant in space, yields the more accurate values  $s \approx 1.7 \pm 0.2$  nm and  $r(0) \approx (1.3 \pm 0.06) \times 10^{-2} \text{ s}^{-1}$  for the off rate at zero force. The latter value is within the error bars of recent x-ray foot printing measurements [20], which also show two time scales for the dissociation of IHF from the DNA. The structural basis for these two different modes of binding is unknown.

*Discussion.*—Protein binding induces large mechanical stresses on the DNA, which can cause large changes of conformation. Bending of the DNA by the IHF protein studied here is an integral part of its function [21,22]. In the cell, DNA is entirely decorated with proteins and under dynamic mechanical stress. The present study provides quantitative measurements of how tension in the DNA affects protein binding. By contrast, most *in vitro* experiments measure binding affinities and rates only at zero tension. The concept of dynamic force spectroscopy, pioneered by Evans and collaborators [17], has been successfully applied to study protein-DNA interactions before [18]. The novelty of the present experiment is the nanometer scale of the DNA probe: by working with 25 nm long DNA, we can detect single local bends and directly measure how rates depend on tension. In addition, our setup is simple enough to form a platform for analytical instrumentation, in contrast to previous single-molecule experiments which involved complex optics and micromanipulation.

In conclusion, we present a simple device to study the binding kinetics of a single protein to a DNA molecule. In the case of IHF, we find a double exponential probability of unbinding. We analyze how mechanical tension in the DNA affects the kinetics. Our method gives access to long time scales and applies to relatively short DNA oligomers of less than 100 bp. It exemplifies a new paradigm of molecular detection, where the target molecule is detected through the conformational change induced in a probe molecule. Here we demonstrate that this allows detection

of single, unlabeled proteins, extending our previous work [9] on detecting single unlabeled DNA oligomers.

We are indebted to Steve Goodman for the gift of the IHF. This work was supported by NSF Grants No. DMR-0105903 and No. DMR-0405632.

- 
- [1] P. A. Rice, S. Yang, K. Mizuuchi, and H. A. Nash, *Cell* **87**, 1295 (1996).
  - [2] K. Svoboda and S. M. Block, *Cell* **77**, 773 (1994).
  - [3] K. Visscher, M. J. Schnitzer, and S. M. Block, *Nature (London)* **400**, 184 (1999).
  - [4] M. D. Wang *et al.*, *Science* **282**, 902 (1998).
  - [5] G. Wuite *et al.*, *Nature (London)* **404**, 103 (2000).
  - [6] T. R. Strick, V. Croquette, and D. Bensimon, *Nature (London)* **404**, 901 (2000).
  - [7] L. Finzi and J. Gelles, *Science* **267**, 378 (1995).
  - [8] B. M. Ali *et al.*, *Proc. Natl. Acad. Sci. U.S.A.* **98**, 10 658 (2001).
  - [9] M. Singh-Zocchi *et al.*, *Proc. Natl. Acad. Sci. U.S.A.* **100**, 7605 (2003).
  - [10] H. Jensenius and G. Zocchi, *Phys. Rev. Lett.* **79**, 5030 (1997).
  - [11] G. Zocchi, *Biophys. J.* **81**, 2946 (2001).
  - [12] D. C. Prieve and N. A. Frej, *Langmuir* **6**, 396 (1990).
  - [13] R. B. Liebert and D. C. Prieve, *Biophys. J.* **69**, 66 (1995).
  - [14] M. Singh-Zocchi, A. Andreasen, and G. Zocchi, *Proc. Natl. Acad. Sci. U.S.A.* **96**, 6711 (1999).
  - [15] M. Daune, *Molecular Biophysics* (Oxford University, New York, 1999).
  - [16] E. Evans, *Faraday Discuss.* **111**, 1 (1999).
  - [17] R. P. Merkle *et al.*, *Nature (London)* **397**, 50 (1999).
  - [18] S. J. Koch and M. Wang, *Phys. Rev. Lett.* **91**, 028103 (2003).
  - [19] See EPAPS Document No. E-PRLTAO-94-085513 for supplementary material, including text and six figures regarding materials and methods. A direct link to this document may be found in the online article's HTML reference section. The document may also be reached via the EPAPS homepage (<http://www.aip.org/pubservs/epaps.html>) or from <ftp.aip.org> in the directory `/epaps/`. See the EPAPS homepage for more information.
  - [20] G. M. Dhavan *et al.*, *J. Mol. Biol.* **315**, 1027 (2002).
  - [21] S. D. Goodman and H. A. Nash, *Nature (London)* **341**, 251 (1989).
  - [22] S. D. Goodman, S. C. Nicholson, and H. A. Nash, *Proc. Natl. Acad. Sci. U.S.A.* **89**, 11 910 (1992).